

# Experimental Investigation and Modeling of Denitrification of Water in a Column Bioreactor using Clinoptilolite Zeolite

## Abstract

The efficiency of nitrate removal in a 9.5 L packed bed column bioreactor was assessed using various feeding strategies and initial concentrations. Zeolite mineral Clinoptilolite particles were employed in the bioreactor to trap and immobilize *Thiobacillus denitrificans*. Different hydraulic retention times were tested to evaluate nitrate removal effectiveness. In the most favorable scenario, there was an 87% reduction in nitrate concentration from an influent of 400 mg/L over a three-hour period. To determine the optimal bioreactor length, a computational fluid dynamics model was created. By comparing simulations with experimental results, the ideal heights for complete denitrification were found to be 90 cm, 45 cm, 30 cm, and 20 cm for influent nitrate concentrations of 400 mg/L, 250 mg/L, 120 mg/L, and 80 mg/L, respectively.

Keywords: Denitrification, Modified Zeolite, Column Bioreactor, CFD

Synopsis: *Thiobacillus denitrificans* is evaluated in a pilot-scale reactor for the first time for its ability to denitrify water containing high sulfur concentrations.

## 1. Introduction

Nitrate is the most common pollutant in water resources of ecosystems. Moreover, its inputs to the environment have been on the rise for the past few decades [1], making the availability of a

24 sustainable source of healthy water increasingly important to many countries because of the  
25 increasing population, expansion of industries, and climate change effects. Various methods are  
26 available for nitrate removal from water, such as reverse osmosis, ion exchange, electrodialysis,  
27 and membrane processes [2-5]. Additionally, there is a rising interest in biological methods [6].  
28 One significant aspect of these biological approaches is microbial denitrification, a respiratory  
29 process carried out by autotrophic and heterotrophic microorganisms [7].

30  
31 The majority of denitrifying microorganisms are heterotrophs, relying on complex organic  
32 substances like methanol, ethanol, methane, carbon monoxide, and acetic acid as electron donors  
33 for the conversion of nitrate to nitrogen [8]. Additionally, some researchers have utilized natural  
34 materials like wheat straw and plant wood as sources of organic carbon for heterotrophic  
35 denitrification. While this method is cost-effective, it comes with a lengthy and intricate pre-  
36 treatment process. In practical applications, for the removal of nitrate from drinking water, simple  
37 and readily degradable substrates like methanol, ethanol, and acetic acid are predominantly utilized  
38 [9].

39  
40 A diverse array of autotrophic bacteria finds application in the denitrification of water with  
41 minimal organic matter content. These microorganisms utilize an inorganic carbon source, such as  
42 CO<sub>2</sub>, as their carbon source [9]. Their advantage lies in not necessitating an external organic  
43 substrate, making them a more cost-effective option [10]. Furthermore, these microorganisms  
44 yield low biomass, thereby minimizing the risk of contamination [1].

45

46 Sulfur-based autotrophic denitrification is a type of denitrification wherein elemental sulfur,  
47 hydrogen sulfide, or thiosulfate serves as electron donors. Certain properties of sulfur make it well-  
48 suited for denitrification, such as its non-toxic nature, insolubility in water, and stability under  
49 normal conditions [10]. However, a few species of microorganisms are capable to reduce nitrate  
50 through oxidizing sulfur elements ( $S^{2-}$ ,  $S_2O_3^{2-}$ ,  $SO_3^{2-}$ ) [11-14]. A number of researchers have  
51 studied the autotrophic denitrification process by *Thiobacillus denitrificans* (enriched sludge or  
52 pure culture) for the removal of nitrate from drinking water, groundwater, and wastewater using  
53 reduced sulfur compounds as electron donors [10, 15-19]. However, only a limited number of  
54 studies have investigated the effectiveness of immobilized *Thiobacillus denitrificans*  
55 Immobilization has the potential to improve denitrification efficiency and safeguard the bacteria  
56 from adverse environmental conditions. The colonization and activation of denitrifying bacteria  
57 communities on supports are critical factors to obtain high denitrification efficiency [20].  
58 Denitrificans can perfectly grow in a packed bed reactor, where the biofilm grows around the fixed  
59 carrier comprised of porous organic matter or mineral matrixes formed by large surface area  
60 particles [1]. There have been many different materials used as bacteria supports in the past, such  
61 as metal oxides [21, 22], zeolites [23], biodegradable polymers [24], woods [25], or carbon  
62 materials [26]. Organic supports, such as polymers, pose various challenges, including issues  
63 related to stability and disposal [27]. Conversely, inorganic materials like silica and alumina  
64 exhibit thermal and mechanical stability, along with robust strength [27]. Furthermore, Battista-  
65 Toledo et al. [28] found that different inorganic materials, like ZSM5, 13X, and b-zeolite, perform  
66 well as bacterial supports for a heterotrophic bacteria called *Escherichia coli*.

67

78 In addition to the characteristics of the supports, environmental parameters such as C/N ratio,  
79 temperature, and pH of polluted water influence the community structure and activity of  
80 denitrifying bacteria. There are several investigations [6, 7, 9, 29-34] on the denitrifying  
81 bioreactors. Torrentó et al. [35] found that nitrate input concentration plays an essential role in the  
82 denitrification efficiency of the reactor. Nitrate removal improves by lowering the initial nitrate  
83 concentration and grain size. According to Carrera et al. [36], denitrification is more efficient at  
84 high temperatures rather than at low temperatures. However, even at low temperatures, the desired  
85 nitrate removal efficiency can be achieved by increasing the hydraulic retention time (HRT). This  
86 parameter is a significant factor that should be considered during the design of a reactor. In a  
87 heterotrophic system, HRT is adjusted based on the growth rate of microorganisms, initial nitrate  
88 concentration, presence of other inhibitory species, and temperature [9].

89  
90 This work aims to investigate the effectiveness of Clinoptilolite zeolite particles as a support for  
91 *Thiobacillus denitrificans* as well as evaluate the performance of a 9.5 L pilot-scale bioreactor  
92 filled with Clinoptilolite zeolite mineral for denitrification process. Furthermore, a computational  
93 fluid dynamics (CFD) model is developed using COMSOL 5.4 software in an attempt to  
94 investigate what the optimal length of the bioreactor would be for a desired HRT. CFD has proven  
95 to be a promising tool to study the flow fields in a reactor and can be successfully applied for  
96 design, redesign, and scale-up purposes in the future. Taking into account the above-mentioned  
97 goals, different feeding strategies, and various initial concentrations of nitrate ions were applied at  
98 various hydraulic retention times.

## 99 **2. Materials and Methods**

## 2.1. Column Bioreactor

The bioreactor used for the denitrification process was a packed bed reactor which was 90% filled with Clinoptilolite zeolite particles of different sizes. Fig. 1 illustrates a schematic picture of this bioreactor, as well as how different particles were arranged inside it. An upward flow was considered for this system to prevent the accumulation of nitrogen and other gases inside the column. Therefore, the inlet to the bioreactor is located at the bottom. Deoxygenated synthetic water (by Nitrogen gas) was pumped from the feeding tank into the column, and it was treated by autotrophic denitrifying microorganisms attached to the zeolite, and exited from the top of the upper portion of the column. The bioreactor was a Plexiglas cylinder, measuring 100 cm in height and 5.5 cm in diameter (9.5 L). It can be seen in Fig. 1 that four ports for liquid samples were installed along the column at 25 cm apart from each other. In addition, two ports were considered for the sampling particles. Larger particles were placed at the bottom, and smaller ones were toward the top of the bed. Change of particle size along the column was considered to increase the contact area as the influent raises in the bioreactor, compensating for lower nitrate concentration due to the denitrification process at the bottom. The characteristics of Clinoptilolite zeolite particles are given in Table 1. Their sizes ranged between 0.4 and 6 mm and had irregular shapes. The average porosity of particles was determined to be 50% and the density ranged between 0.5 and 1.1 kg. m<sup>-3</sup>.

## 2.2. Zeolite Modification

Before starting the test and in order to remove surface impurities, zeolite particles were washed with water for 48 hours and then dried in an oven at 105 °C for 48 hours. Then, 20 vol.% hydrochloric acid was applied for four hours, followed by extensive washing with distilled water

114 until pH 6 was reached in the effluent. The particles were then dried in an oven at 105 °C for 48  
115 hours. The color of zeolite became brighter after modification by acid.

116

### 117 2.3. Microbiological Culture

118 This investigation was part of a bigger plan for denitrification of water containing nitrite and sulfur  
119 elements in large scales. In this regard, *Thiobacillus* microorganism (ATCC 23644 Gram-negative)  
120 was used for the simultaneous elimination of nitrite and sulfur. The microorganism was obtained  
121 from the German DSMZ microbial collection. This microorganism utilizes sulfur for energy  
122 (hydrogen sulfide, elemental sulfur, or thiosulfate) and requires a pH of 7 and a temperature of 30  
123 °C for optimum growth. *Thiobacillus denitrificans* were cultivated on a basal salt medium (BSM)  
124 which was prepared in three separate and isolated parts. The composition of BSM is presented in  
125 Table 2. Compounds containing phosphorus and chlorine were esterified separately. An autoclave  
126 was used to sterilize all the ingredients of the culture medium for 20 minutes at 121 °C and 1.5  
127 atm pressure. Once the sterile solutions were removed from the autoclave, they were cooled down  
128 to 50 °C, mixed together, and divided into sterile vials. The strains were mixed using a flame and  
129 sterilized syringe under the biological hood, then inoculated into the vials at a rate of 10% and  
130 incubated at 30 °C for one week. The stored microorganism cultures were transferred to the new  
131 environment on a monthly basis and the new cultures replaced the previous ones. To avoid  
132 interference from photoautotrophic microorganisms, aluminum foil was used to cover the column,  
133 preventing the penetration of light into the system.

134

### 135 2.4. Operational Plan

136 The operating plan for this investigation is reported in Table 3. The whole operation took about 4  
137 months, and sampling for physicochemical properties was performed 2 to 3 times per week from  
138 the designated ports. There were three phases in the operational plan, each with a different  
139 objective. Detailed descriptions of each phase are provided below.

140  
141 Before starting the process and in order to reach a usable level of cell population in the column  
142 inoculation, 5 L of BSM was inoculated by *Thiobacillus denitrificans*. It was incubated in an  
143 Erlenmeyer flask at 30 °C under sterile conditions for 30 days. The number of cells was counted  
144 under an optical microscope to ensure the growth and division of cells. Also, every week, 10% of  
145 the medium was replaced with a fresh BSM.

146  
147 The first stage (set-up) involved adding 4 L *Thiobacillus denitrificans* medium from the  
148 discontinuous culture, and 6 L of non-sterile BSM to the reactor inlet. The reactor operated in a  
149 closed loop in order to provide sufficient contact time between cells, nutrients and substrate.  
150 During this period, 1 L of fresh BSM was added to an influent nitrate concentration of 550 mg. L<sup>-1</sup>  
151 each day. It should be mentioned that until the 6<sup>th</sup> day (end of set-up stage), the HRT was set to  
152 25 hours and to 32 hours afterward. The hydraulic retention time was calculated as follows:

$$HRT = \frac{\text{Pore bed volume}}{\text{Flow rate}} = \frac{V\varepsilon}{Q} \quad (1)$$

153 where  $V$  is the volume of the bed,  $\varepsilon$  is the porosity, and  $Q$  is the flow rate.

154  
155 In the growth and incubation stage, the reactor cycle was changed from closed to open to form the  
156 microbial biofilm and the column was treated with a BSM containing 550 mg. L<sup>-1</sup> nitrate ion. The  
157 concentration of nitrate ions was measured each day to monitor its significant reduction in the

108 effluent. This reduction indicated that the bioreactor was ready for the gradual replacement of  
109 BSM with synthetic water (SW). The compounds present in different concentrations of synthetic  
110 water (SW) are given in Table 4.

111  
112 Finally, once the denitrification rate remained stable and the column reached the steady-state  
113 condition, feeding experiments were carried out and the performance of the column in removing  
114 nitrate ions was evaluated based on different nitrate input concentrations and HRTs. The feeding  
115 experiments started from the longest hydraulic retention time (25 hours) and shorter HRTs were  
116 employed based on the reactor performance and standard limits for nitrite and nitrate ions in the  
117 effluent. It is worth mentioning that with increasing nitrate ion concentration, alkaline and  
118 thiosulfate ion values also increase. Therefore, the pH of the environment was adjusted in the  
119 range of 7.7-8 using 2 molar NaOH solution.

### 119 **3. Physicochemical Analyses**

#### 120 **3.1. Nitrate Test**

121 In this study, the Chromotropic Acid method was employed to quantify nitrate levels, with the  
122 specified range for nitrogen being 1-130 mg/L. The underlying principle of this method involves  
123 the creation of a yellow solution through the reaction of Nitrate Reagent A and Nitrate Reagent B  
124 with nitrate. Subsequently, the absorbance of the resulting solution was measured using a  
125 spectrophotometer at a wavelength of 410 nm. To establish the nitrate standard curve, varying  
126 concentrations of nitrate solution were prepared using potassium nitrate. Each test tube containing  
127 Nitrate Reagent A received 1 ml of nitrate solution, and the tube was shaken 10 times. Following  
128 that, Nitrate Reagent B was added to each tube through a funnel, and the tubes were shaken another



181 10 times. Once the yellow color fully developed, a specific volume of the solution was withdrawn  
182 using a Pasteur pipette and transferred to the cuvette. The device was initially calibrated with  
183 nitrate-free distilled water, and the absorbance of each test tube was then read at a wavelength of  
184 410 nm to establish the nitrate standard curve.

185  
186 To measure nitrate in the samples after obtaining the nitrate standard curve, cells were separated  
187 from the culture medium through centrifugation at 5000 rpm for 20 minutes. After passing the  
188 samples through a 0.45-micron filter paper and conducting the dilution process, one milliliter of  
189 the resultant solution was transferred to a test tube containing Nitrate Reagent A, followed by 10  
190 shakes. Subsequently, Nitrate Reagent B was introduced into the test tube using a funnel, and the  
191 tube was shaken another 10 times until the yellow color fully manifested. Spectrophotometer data  
192 and absorbance changes were then compared with the absorption standard curve, ultimately  
193 yielding the nitrate concentration.

### 194 195 **3.2. Nitrite Test**

196 To quantify nitrite levels, the USEPA Diazotization method was employed with a measurement  
197 range of 0.002-0.03 mg/L of nitrogen. The methodology involves creating nitrite solutions using  
198 sodium nitrite at various concentrations. Subsequently, Nitrite Reagent is introduced to 10 ml of  
199 these solutions using a funnel, followed by shaking the tubes 10 times. After approximately 20  
200 minutes, a pink coloration develops. A specific volume of the solution is then extracted using a  
201 Pasteur pipette and transferred to a cuvette. The instrument is initially calibrated to zero using  
202 distilled water devoid of nitrite. Subsequently, the absorbance of the samples is read at a  
203 wavelength of 507 nm, and a nitrite standard curve is generated. The method relies on the reaction

204 of nitrite with sulfonic acid, forming diazonium salt and producing a pink color. After establishing  
205 the nitrite standard curve, cells were separated from the culture medium via centrifugation at 5000  
206 rpm for 20 minutes. Following filtration through a 0.45-micron filter paper and necessary dilution  
207 steps, 10 mL of the upper solution was combined with the Nitrite Reagent using a funnel. After  
208 shaking the tubes and the complete development of the pink color, the absorbance of the samples  
209 was measured at a wavelength of 507 nm. Spectrophotometer data and absorption changes were  
210 then compared with the absorption standard curve to determine the nitrite concentration.

211

### 212 3.3. pH Test

213 The pH of the samples was instantly measured using a digital pH meter, without filtration or  
214 dilution, immediately after sampling.

215

### 216 3.4. Characterization of Zeolite Particles

217 In order to characterize the zeolite particles used in the research, scanning electron microscope  
218 (SEM) images were used to study the surface structure and morphology. Also, to determine the  
219 elemental composition of samples, energy dispersive X-ray (EDX) method was used at room  
220 temperature. In this method, the surface of the sample is bombarded by an electron beam inside  
221 the microscope, and when the electrons of this beam collide with the electrons of the atoms of the  
222 sample under investigation, some of these electrons are displaced. Due to the fact that the place of  
223 atoms cannot remain empty and must reach the equilibrium state, electrons from higher atomic  
224 layers migrate to this empty place and fill its place. In order to perform this action, the electrons  
225 of the higher layers, which have more energy, must lose some of their energy to reach the energy  
226 level of the new layer and be stable, and this energy is emitted as X-rays.

۲۲۷

۲۲۸ The magnitude of energy emitted depends on the specific layers involved—both the layer from  
۲۲۹ which the electron is detached and the layer to which it migrates. Additionally, each element's X-  
۲۳۰ rays emit a distinct amount of energy during the transition from one atomic layer to another.  
۲۳۱ Consequently, by quantifying the energy in X-rays released during electron beam bombardment,  
۲۳۲ it becomes feasible to discern the type of atom within the sample. The outcome of an EDX analysis  
۲۳۳ is a spectrum, where the displayed peaks are unique to individual atoms, signifying the presence  
۲۳۴ of a specific element.

۲۳۵

#### ۲۳۶ 4. Computational Fluid Dynamics Model Development

۲۳۷ COMSOL Multiphysics 5.4 software was utilized for generating the bioreactor configuration,  
۲۳۸ meshing, and solving the governing equations using the finite element method. To obtain the flow  
۲۳۹ profiles inside the bed, fluid properties were considered as water. Such an assumption is reasonable  
۲۴۰ due to the low nitrate concentration in water.

۲۴۱

##### ۲۴۲ 4.1. Governing Equations

۲۴۳ The governing equations for the porous fixed bed bioreactor are:

$$\frac{\partial}{\partial t}(\epsilon_p \cdot \rho) \nabla \cdot (\rho \cdot u) = Q \quad (2)$$

$$u = -\frac{K}{\mu} \nabla \rho \quad (3)$$

۲۴۴ where  $\epsilon_p$  is the porosity of the bed,  $\rho$  is the density of the fluid,  $u$  is velocity,  $K$  is the permeability,  
۲۴۵ and  $\mu$  is the viscosity.

۲۴۶

247 The equation of mass transfer for species  $i$  in the reactor, which includes diffusion, convection and  
248 chemical reaction, is as follows:

$$\frac{\partial S_i}{\partial t} + \nabla \cdot (-D_i \nabla S_i) + \nabla \cdot (\vec{u} S_i) = R_i \quad (4)$$

249 where  $t$  is time,  $S_i$  is concentration of species  $i$ ,  $D_i$  is diffusion coefficient of the species  $i$ ,  $\vec{u}$  is  
250 velocity, and  $R_i$  is chemical reaction rate for the species  $i$ .

251

## 252 4.2. Reaction Kinetics

253 To describe the denitrification process in this study, the Monod equation was used:

$$r_s = -\frac{\mu_m S}{K_s + S} \quad (5)$$

254 where  $r_s$  is the growth rate of microorganism,  $\mu_m$  is the maximum growth rate of microorganism,  
255  $K_s$  is the half-velocity constant, and  $S$  is the concentration of the substrate for growth.

256

## 257 4.3. Model Configuration

258 To reach comparable results with experimental data, a 9.5 L cylindrical bioreactor was generated  
259 with the same height and diameter as actual setup. Then, the generated geometry was meshed using  
260 tetrahedral mesh elements. The generated mesh used for CFD simulations is shown in Fig. 2. As  
261 the concentration of the nitrate drops by going upward through the bioreactor, four different mesh  
262 sizes were applied ranging from coarse at the inlet to fine at the outlet to acquire precise results.

263

264 It was considered that the influent enters the bioreactor with a fixed velocity ( $u_0$ ) and concentration  
265 ( $S_{0i}$ ) in the simulation. The velocity was calculated based on the residence time of the fluid. Table  
266 5 summarizes the values and parameters used for the simulation based on the experimental values.

Due to the low concentration of nitrate in water, the physical properties of the fluid in the reactor were considered to be the same as water at 30 °C.

## 5. Results and Discussion

### 5.1. Zeolite Modification

The mineral morphology of water-washed zeolite, acid-modified zeolite, and zeolite-microorganism were assessed using scanning electron microscopy (SEM). Figs 3, 4, and 5 display SEM images of water-washed zeolite, acid-modified zeolite, and zeolite-biofilm, respectively, at various magnifications.

Upon comparing acid-modified zeolite with natural zeolite, it is evident that acid modification results in more significant and larger pores. This augmentation enhances the specific surface area of the zeolite, facilitating the formation of microbial biofilm. Fig. 5 presents the SEM imaging results of particles after development of microbial biofilm. As depicted in the figure, the microbial cells exhibit a bacilli shape, with lengths ranging from 0.5 to 1.4  $\mu\text{m}$ , mirroring the findings of the study conducted by Gu et al. [37]. The dimensions of the microorganisms captured in the images align entirely with those of *Thiobacillus denitrificans*.

Furthermore, the EDX results for both natural zeolite and modified zeolite are depicted in Figs. 6 and 7, along with corresponding data presented in Tables 6 and 7, respectively. Based on the EDX findings, the Si/Al ratio in natural zeolite is 5.45, while in acid-washed zeolite, it has increased to 11.75. In a study conducted by Shirazi et al. [38], SEM results revealed that zeolite with varying Si/Al ratios exhibits distinct morphologies and pore sizes. Surface area measurement demonstrated

290 that reducing the Si/Al ratio leads to a decrease in the zeolite's surface area [68]. Additionally, the  
291 acidity analysis of synthetic zeolite indicated that different Si/Al ratios impact the surface acidity,  
292 which consequently impact microorganism immobilization. Therefore, the acid-modified zeolite  
293 with a higher Si/Al ratio possesses an increased surface area, enhancing the optimal conditions for  
294 biofilm formation.

295

## 296 5.2. Experimental Measurements

297 Fig. 8 shows the whole denitrification process, including set-up, growth, and feeding stages with  
298 different HRTs. It also shows nitrate concentrations in the influent and effluent, and the removal  
299 efficiency during these periods. As mentioned above, during the set-up and growth stages (Fig.  
300 8a), a constant 550 mg. L<sup>-1</sup> concentration of nitrate was introduced to the bioreactor. In the set-up  
301 which lasted 7 days, the bioreactor had a negative efficiency and the concentration of nitrate in the  
302 effluent was higher than in the influent. This negative efficiency happened due to the conversion  
303 of ammonium ions into nitrate during this period. Between days 7 to 30 (the growth stage), the  
304 nitrate concentration gradually decreased in the outlet, indicating the growth and stabilization of  
305 autotrophic microorganisms in the bioreactor. Finally, the bioreactor reached an exploitation level  
306 in less than 22 days and the denitrification process could be started from this day. However, the  
307 stabilization process continued till day 30 to increase the population growth and the efficiency of  
308 the bioreactor. It is worth noting that the set-up and growth times in different systems only depend  
309 on the type and size of the bioreactor and the type of microorganisms. Thus, different times are  
310 reported in different research for these stages [15, 39, 40].

311

312 In the feeding stages (Figs. 8b to 8g), the performance of the bioreactor was tested at different  
313 HRTs (25, 15, 12, 10, 6 and 3 hours) and various nitrate input concentrations for each HRT (400,  
314 250, 120 and 80 mg. L<sup>-1</sup>). As expected, the efficiency of the bioreactor increased by lowering the  
315 input concentration in each HRT which is due to the strengthening of the biofilm and population  
316 growth on particles during the operation of the bioreactor.

317  
318 Comparing different HRTs, the outlet concentrations of nitrate were always below the standard  
319 value (45 mg. L<sup>-1</sup>) for the influents with nitrate concentrations of 120 and 80 mg. L<sup>-1</sup>. Thus, it can  
320 be said that these concentrations are less than the potential power of the bioreactor in the intended  
321 HRTs. In the case of the influent with a concentration of 250 mg. L<sup>-1</sup>, the effluent nitrate  
322 concentration was always below or near the standard level in all HRTs, ensuring that higher nitrate  
323 inputs are feasible. However, for the influent with a nitrate concentration of 400 mg. L<sup>-1</sup>, the  
324 efficiency of the bioreactor was considerably low, and the output nitrate concentrations were  
325 higher than the standard limit in all HRTs. To overcome this problem without increasing the HRT,  
326 a nitrate shock was applied to the bioreactor by injecting the synthetic influent with a nitrate  
327 concentration of 1500 mg. L<sup>-1</sup>. This shock was like a new growth in the incubation stage for the  
328 bioreactor and was applied between days 95 and 101 with a 3-hour HRT. This shock significantly  
329 increased the uptake of nutrients and the efficiency of the bioreactor, such that the effluent nitrate  
330 concentration for the 400 mg. L<sup>-1</sup> influent reached 44 mg. L<sup>-1</sup>, just below the standard value.  
331 Overall, the efficiency of the bioreactor was always above 50% and in a constant range of 59-68%  
332 in different HRTs for the influent with a concentration of 400 mg. L<sup>-1</sup>. However, after the nitrate  
333 shock on the 104th day of the operation, a significant increase was observed in the efficiency of  
334 nitrate removal up to 87%, which can be the result of microorganism cell growth and the increased

number of cells. Zhao et al. [33] also reached 90% nitrate removal efficiency in a 3-hour HRT. However, the initial concentration of nitrate and the volume of the bioreactor were much lower than in the current study.

In this work, the main concern about the effluent quality was the concentration of nitrate and nitrite ions. Therefore, these two concentrations were measured every 1 to 3 days. Fig. 9 shows the concentration profile of the input nitrate, output nitrate and output nitrite ions at different HTRs throughout the entire duration of the operation of the bioreactor. It can be seen in this figure that the amount of nitrite in the outlet was always below the standard limit ( $3 \text{ mg. L}^{-1}$ ), except in the growth and the nitrate shock phases. Nitrate was incompletely reduced in these phases due to the higher concentrations rather than the standard capacity of the bioreactor.

### 5.3. CFD Simulations

The precision of simulation results strongly depends on the quality and size of meshes. In order to determine the proper element size, computational error of nitrate removal was calculated for each mesh size by considering the difference between experimental data and simulation results. Fig. 10 shows the error nitrate removal efficiency for different mesh sizes named by their number of elements. According to this figure, as the error does not decrease with further decreasing of the size of elements, the mesh with 155661 elements was selected for performing the simulations.

To ensure the reliability of CFD results, the same scenario as the experimental test was applied, with the exception that there was no need for the set-up and growth stages. An excellent agreement between the experimental data of growth rate and the prediction of Eq. (5) was observed.



358 Maximum growth of microorganisms ( $\mu_m$ ) and half-velocity constant ( $K_s$ ), which are shown in  
359 Table 8, were calculated through monod equation linearization [41] and applying the least-square  
360 method on nitrate concentrations at influent and effluent.

361  
362 The comparison of CFD simulation results with experiments is shown in Fig. 11. A good  
363 agreement between the experimental and simulated values can be seen in this figure and the  
364 relative error can be attributed to the environmental factors such as temperature oscillations in the  
365 experiment. Furthermore, the presence of other minerals which affect the active surface of the  
366 particles has not been taken into account in the simulations. These minerals fill the empty space of  
367 the particles and reduce the mass transfer rate for nitrate absorption.

#### 368 369 **5.4. Optimal Reactor Height Determination**

370 CFD simulation was utilized for further understanding of the bioreactor performance as an  
371 alternative for the time demanding and costly experiments. Fig. 12 shows the profile of nitrate  
372 concentration along the bioreactor for various initial concentrations in the 3-hour retention time.  
373 The main purpose of this investigation is to reach the maximum nitrate removal with the minimum  
374 HRT and reactor volume. It can be seen in this figure that for the influent with 400 mg. L<sup>-1</sup> nitrate  
375 concentration, the bioreactor length is optimal and the effluent concentration has reached the  
376 standard level at the end of the packed bed (90 cm). However, for the influents with 250, 120 and  
377 80 mg. L<sup>-1</sup> of nitrate concentration, the standard level could be obtained at 45, 30 and 20 cm of the  
378 reactor length.

#### 379 **6. Conclusions**

380 The effectiveness of nitrate removal was assessed in a 9.5 L packed bed column bioreactor through  
381 the evaluation of various feeding strategies and initial concentrations. The bioreactor was filled  
382 with zeolite mineral particles modified through acid washing process. Acid washing increased the  
383 pore size of zeolite particles compared to natural zeolite which facilitates the formation of  
384 microbial biofilm. Multiple hydraulic retention times were investigated to determine the efficiency  
385 of nitrate removal. The results demonstrate that the designed bioreactor is capable of achieving an  
386 87% reduction in nitrate levels within a three-hour timeframe. This indicates that the bioreactor  
387 system can effectively remove nitrate ions from water, even when the initial nitrate content is as  
388 high as 400 mg/L, which exceeds the standard limit of 45 mg/L. The computational fluid dynamics  
389 (CFD) model yielded satisfactory results, confirming the effectiveness of the bioreactor design. It  
390 revealed that the optimal length of the bioreactor is suitable for influents containing 400 mg/L of  
391 nitrate. However, for influents with lower nitrate concentrations or when employing lower  
392 hydraulic retention times (HRTs), the bioreactor can be constructed with shorter heights. The CFD  
393 model can serve as a valuable tool for future studies, particularly in scaling up the bioreactor  
394 system.

395  
396 Considering the fact that nitrate-contaminated wastewater usually contains COD, N and P  
397 simultaneously, further research is needed to investigate the performance of the presented system  
398 in this regard. Furthermore, performing microbial community analysis is highly recommended for  
399 the future works to investigate the possibility of microbial consortium instead of Thiobacillus  
400 denitrificans alone [42].

401

## 402 7. Nomenclature

### Abbreviations

<b>BSM</b>	<b>Basal Salt Medium</b>
<b>CFD</b>	<b>Computational Fluid Dynamics</b>
<b>EDX</b>	<b>Energy Dispersive X-ray</b>
<b>HRT</b>	<b>Hydraulic Retention Times</b>
<b>SEM</b>	<b>Scanning Electron Microscope</b>
<b>SW</b>	<b>Synthetic Water</b>

### Symbols

$D_i$	Diffusion coefficient ( $\text{m}^2 \cdot \text{s}^{-1}$ )
$K$	Bed permeability (s)
$K_s$	Half-growth rate constant ( $\text{kg} \cdot \text{m}^{-3}$ )
$n$	Normal unit vector
$Q$	Flow rate ( $\text{m}^3 \cdot \text{h}^{-1}$ )
$R_i$	Reaction rate ( $\text{kg} \cdot \text{m}^{-3} \cdot \text{s}^{-1}$ )
$r_s$	Concentration change ( $\text{kg}/\text{m}^3 \cdot \text{s}$ )
$S_i$	Nitrate concentration of species $i$ ( $\text{kg} \cdot \text{m}^{-3}$ )
$S_0$	Inlet nitrate concentration ( $\text{kg} \cdot \text{m}^{-3}$ )
$t$	Time (s)
$u$	Velocity ( $\text{m} \cdot \text{s}^{-1}$ )
$u_0$	Inlet velocity ( $\text{m} \cdot \text{s}^{-1}$ )
$V$	Bed volume ( $\text{m}^3$ )

*Greek letters*

$\varepsilon$	Porosity of bed
$\rho$	Density (kg. m <sup>-3</sup> )
$\mu$	Viscosity (Pa.s)
$\mu_m$	Specific growth rate (s <sup>-1</sup> )

ε.ε

ε.ε

Accepted manuscript

**Table 1.** Properties of zeolite particles

<b>Size (mm)</b>	0.4 – 6
<b>Shape</b>	Irregular
<b>Particle Porosity (%)</b>	50
<b>Density (kg/m<sup>3</sup>)</b>	0.5 – 1.1

ε.ο

ε.γ

Accepted manuscript

ε.γ

**Table 2.** BSM compositions

<b>Chemical Formula</b>	<b>Amount</b>
KH <sub>2</sub> PO <sub>4</sub>	1.8 (g/L)
Na <sub>2</sub> HPO <sub>4</sub>	1.2 (g/L)
MgSO <sub>4</sub> .7H <sub>2</sub> O	0.1 (g/L)
(NH <sub>4</sub> ) <sub>2</sub> SO <sub>4</sub>	0.1 (g/L)
CaCl <sub>2</sub> .2H <sub>2</sub> O	0.03 (g/L)
Na <sub>2</sub> S <sub>2</sub> O <sub>3</sub> .5H <sub>2</sub> O	15 (g/L)
FeCl <sub>3</sub> .6H <sub>2</sub> O	0.02 (g/L)
MnSO <sub>4</sub>	0.02 (g/L)
NaHCO <sub>3</sub>	0.5 (g/L)
KNO <sub>3</sub>	5 (g/L)
EDTA	0.0005 (g/L)
ZnSO <sub>4</sub> .7H <sub>2</sub> O	0.0001 (g/L)
CuCl <sub>2</sub> .2H <sub>2</sub> O	0.00001 (g/L)
MnCl <sub>2</sub> .4H <sub>2</sub> O	0.00003 (g/L)
CoCl <sub>2</sub> .6H <sub>2</sub> O	0.0002 (g/L)
Na <sub>2</sub> MO <sub>7</sub> O <sub>24</sub> .2H <sub>2</sub> O	0.00003 (g/L)
FeSO <sub>4</sub> .7H <sub>2</sub> O	0.0002 (g/L)
H <sub>3</sub> BO <sub>3</sub>	0.0003 (g/L)
NiCl <sub>2</sub> .6H <sub>2</sub> O	0.00002 (g/L)

ε.α

ε.ρ

Accepted manuscript

**Table 3.** Operational plan of the column bioreactor

Stage	Target	Culture Medium	HRT (h)	Nitrate Input Concentration (mg/L)	Days
<b>Setting up</b>	Growth of Autotrophic Microorganisms	BSM	25	1500	1-6
			32	1500	
<b>Growth and Incubation</b>	Biofilm Formation	BSM/Synthetic Water	32	550	7-30
			25	400	31-44
				250	
				120	
				80	
			15	400	45-61
				250	
				120	
				80	
			12	400	62-75
				250	
				120	
80					
<b>Feeding</b>	Performance Evaluation	Synthetic Water	10	400	76-85
				250	
				120	
				80	
			6	400	86-98
				250	
				120	
				80	
			3	1500	99-113
				1500	
				400	
				250	
				120	
				80	

Accepted manuscript

٤١٣

٤١٤

**Table 4.** components of SW for different nitrate ion concentrations (in mg/L)

Nitrate Input Concentration (mg/L)	Chemical Formula						
	KNO <sub>3</sub>	NaHCO <sub>3</sub>	K <sub>2</sub> HPO <sub>4</sub>	NH <sub>4</sub> Cl	MgCl <sub>2</sub> .6H <sub>2</sub> O	FeSO <sub>4</sub>	Na <sub>2</sub> S <sub>2</sub> O <sub>3</sub> .5H <sub>2</sub> O
80	130	250	20	12	2	1	10
120	250	350	50	12	2	1	160
250	434	750	50	12	2	1	350
400	652	1200	50	12	2	1	550
550	901	1700	50	12	2	1	750
1500	2440	4000	50	12	2	1	2000

٤١٥

٤١٦

Accepted manuscript



417

**Table 5.** Parameters used in CFD simulations

<b>Parameter</b>	<b>Symbol</b>	<b>Value</b>	<b>Unit</b>
<b>Fluid residence time</b>	$T_{av}$	3	h
<b>Nitrate molecular weight</b>	Mw	62.0049	g/mol
<b>Concentration of nitrate at inlet</b>	$S_0$	400-80	mg/L

418

419

Accepted manuscript

٤٢٠

**Table 6.** Results of EDX analysis on natural zeolite

Element	Line	Int	Error	K	Kr	W%	A%	ZAF
C	Ka	12.2	3.4065	0.0259	0.0132	8.40	12.89	0.1574
N	Ka	5.5	3.4629	0.0162	0.0083	3.53	4.65	0.2343
O	Ka	360.1	3.5192	0.3740	0.1907	50.41	58.08	0.3782
Na	Ka	15.5	3.6881	0.0059	0.0030	0.58	0.47	0.5112
Mg	Ka	1.5	3.7444	0.0005	0.0003	0.04	0.03	0.6644
Al	Ka	229.0	3.8007	0.0783	0.0399	5.31	3.63	0.7523
Si	Ka	1270.0	3.8570	0.4540	0.2315	28.95	19.00	0.7997
K	Ka	58.7	0.4875	0.0365	0.0186	2.23	1.05	0.8330
Ca	Ka	4.2	0.4941	0.0029	0.0015	0.17	0.08	0.8605
Fe	Ka	3.4	0.2561	0.0057	0.0029	0.37	0.12	0.7934
				1.0000	0.5099	100.00	100.00	

٤٢١

٤٢٢

٤٢٣

٤٢٤

٤٢٥

٤٢٦

٤٢٧

٤٢٨

٤٢٩

٤٣٠

٤٣١

٤٣٢

٤٣٣

٤٣٤

٤٣٥

٤٣٦

٤٣٧

٤٣٨

٤٣٩

٤٤٠

٤٤١

٤٤٢

**Table 7.** Results of EDX analysis on modified zeolite

<b>Eeement</b>	<b>Line</b>	<b>Int</b>	<b>Error</b>	<b>K</b>	<b>Kr</b>	<b>W%</b>	<b>A%</b>	<b>ZAF</b>
<b>C</b>	Ka	13.1	3.4396	0.0227	0.0118	7.38	11.17	0.1596
<b>N</b>	Ka	7.3	3.4964	0.0176	0.0092	3.59	4.66	0.2551
<b>O</b>	Ka	500.9	3.5533	0.4240	0.2201	54.65	62.10	0.4029
<b>Na</b>	Ka	0.0	0.0000	0.0000	0.0000	0.00	0.00	0.4998
<b>Mg</b>	Ka	1.1	3.7807	0.0003	0.0002	0.02	0.02	0.6578
<b>Al</b>	Ka	133.7	3.8375	0.0373	0.0194	2.59	1.74	0.7477
<b>Si</b>	Ka	1635.5	3.8944	0.4766	0.2474	30.43	19.70	0.8133
<b>K</b>	Ka	37.4	0.2685	0.0189	0.0098	1.18	0.55	0.8303
<b>Ca</b>	Ka	1.3	0.2721	0.0007	0.0004	0.05	0.02	0.8600
<b>Fe</b>	Ka	1.3	0.1572	0.0018	0.0009	0.12	0.04	0.7904
				1.0000	0.5192	100.00	100.00	

٤٤٣

٤٤٤

٤٤٥

٤٤٦

٤٤٧

٤٤٨

٤٤٩

٤٥٠

٤٥١

٤٥٢

٤٥٣

٤٥٤

٤٥٥

٤٥٦

٤٥٧

٤٥٨

٤٥٩

٤٦٠

٤٦١

٤٦٢

Accepted manuscript

463

464

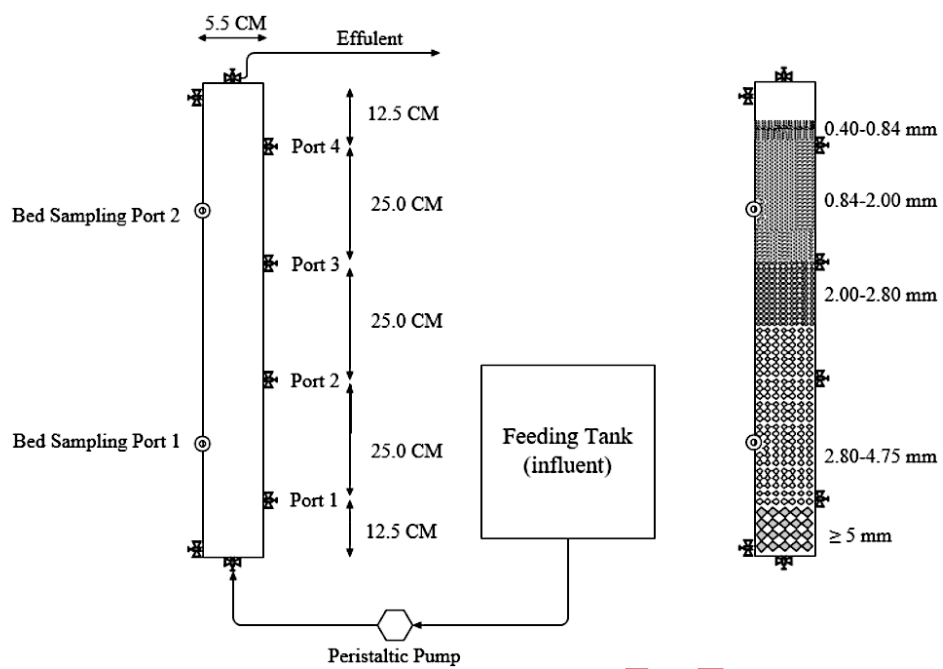
**Table 8.** Constants of Monod equation

$\mu_m$ (mg NO <sub>3</sub> <sup>-</sup> . gh <sup>-1</sup> )	12.7
$K_s$ (mg NO <sub>3</sub> <sup>-</sup> . L <sup>-1</sup> )	0.47

465

466

Accepted manuscript



٤٦٧

٤٦٨ **1 . Fig.** Schematic of the column bioreactor and arrangement of the beds of different sizes of particles

٤٦٩

Accepted manuscript

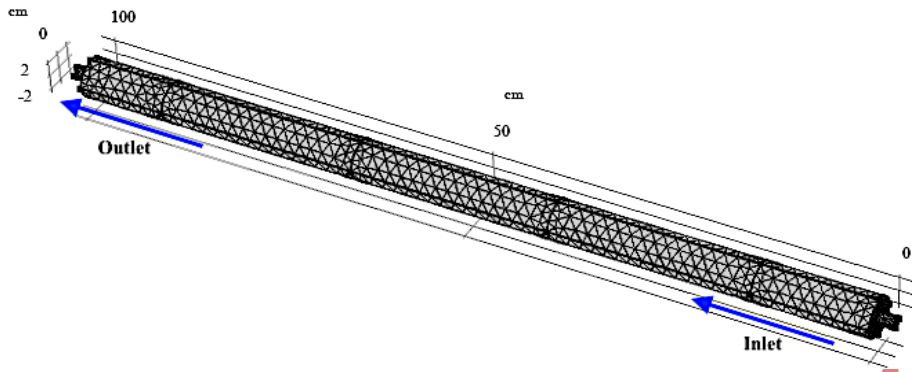


Fig. 2. Schematic of tetrahedral meshes in the bioreactor

470

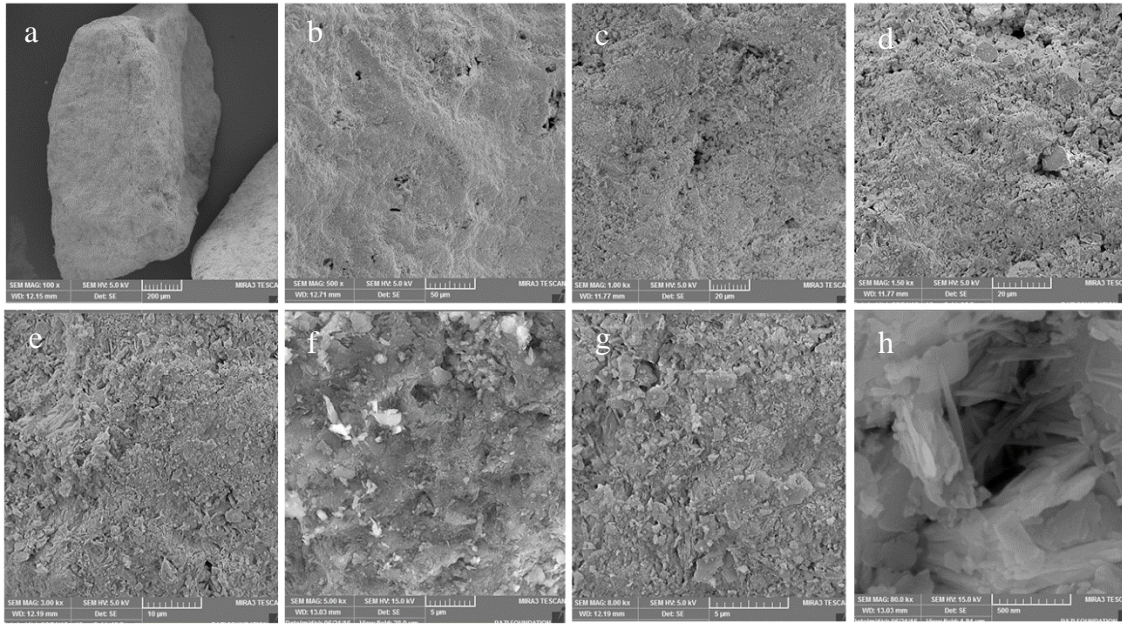
471

472

473

Accepted manuscript

474



475

476

477

478

479

480

481

482

483

484

485

486

487

488

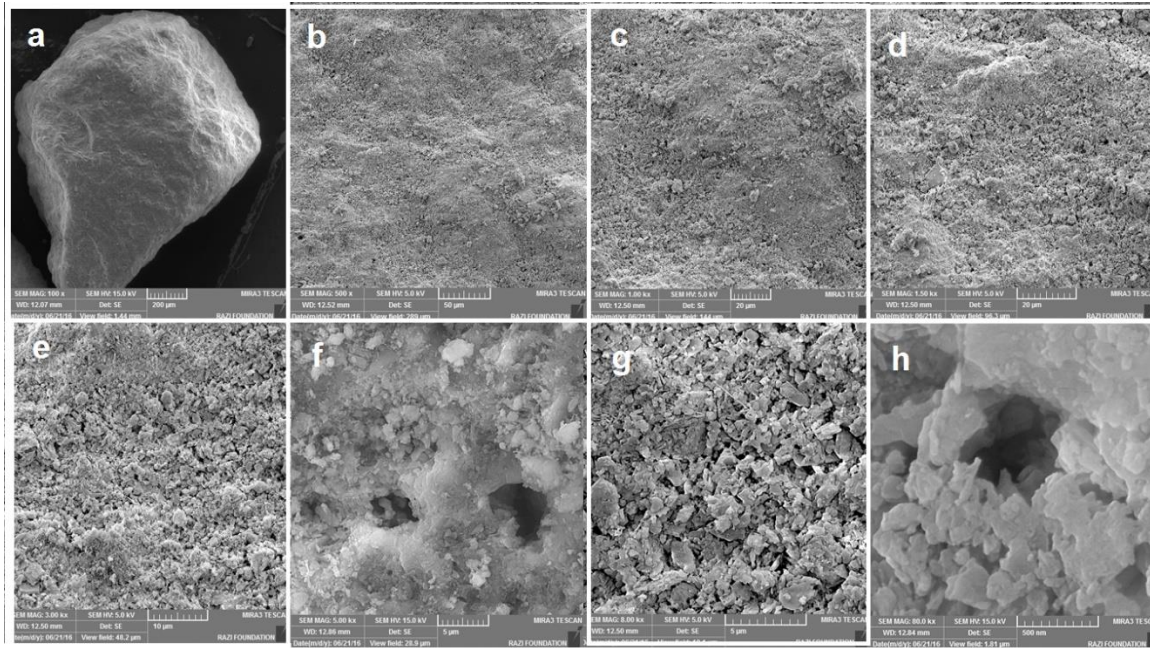
489

**Fig. 3.** SEM image of natural zeolite a) Magnification 100, b) Magnification 500, c) Magnification 1000, d)

Magnification 1500, e) Magnification 3000, f) Magnification 5000, g) Magnification 8000, h) Magnification 80000

Accepted manuscript

٤٩٠



٤٩١

٤٩٢

٤٩٣

٤٩٤

٤٩٥

٤٩٦

٤٩٧

٤٩٨

٤٩٩

٥٠٠

٥٠١

٥٠٢

٥٠٣

٥٠٤

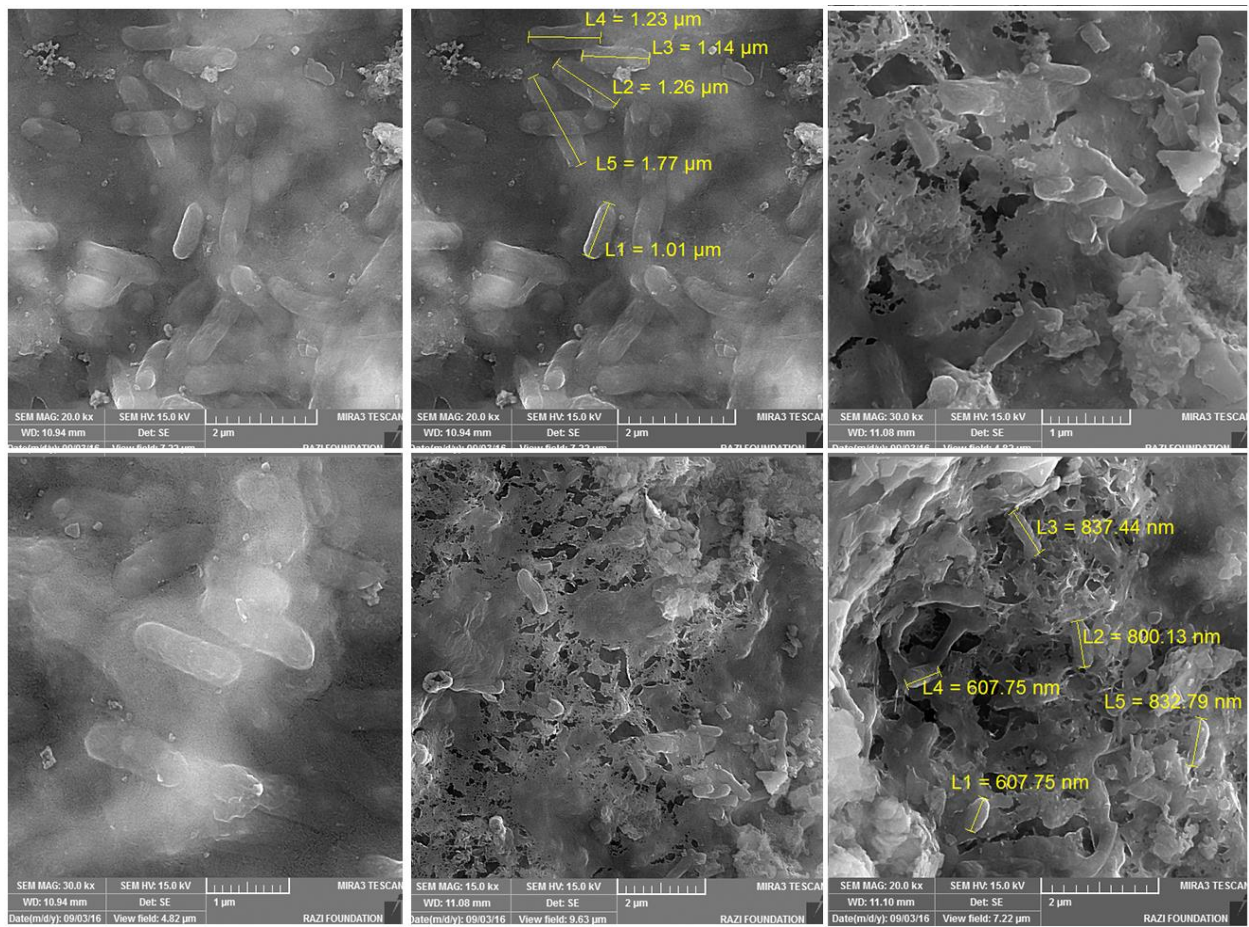
٥٠٥

**Fig. 4.** SEM image of modified zeolite a) Magnification 100, b) Magnification 500, c) Magnification 1000, d) Magnification 1500, e) Magnification 3000, f) Magnification 5000, g) Magnification 8000, h) Magnification



0.6

0.7



0.8

0.9

0.10

0.11

0.12

0.13

0.14

0.15

0.16

0.17

**Fig. 5. SEM image of zeolite-microorganism after development of microbial biofilm**

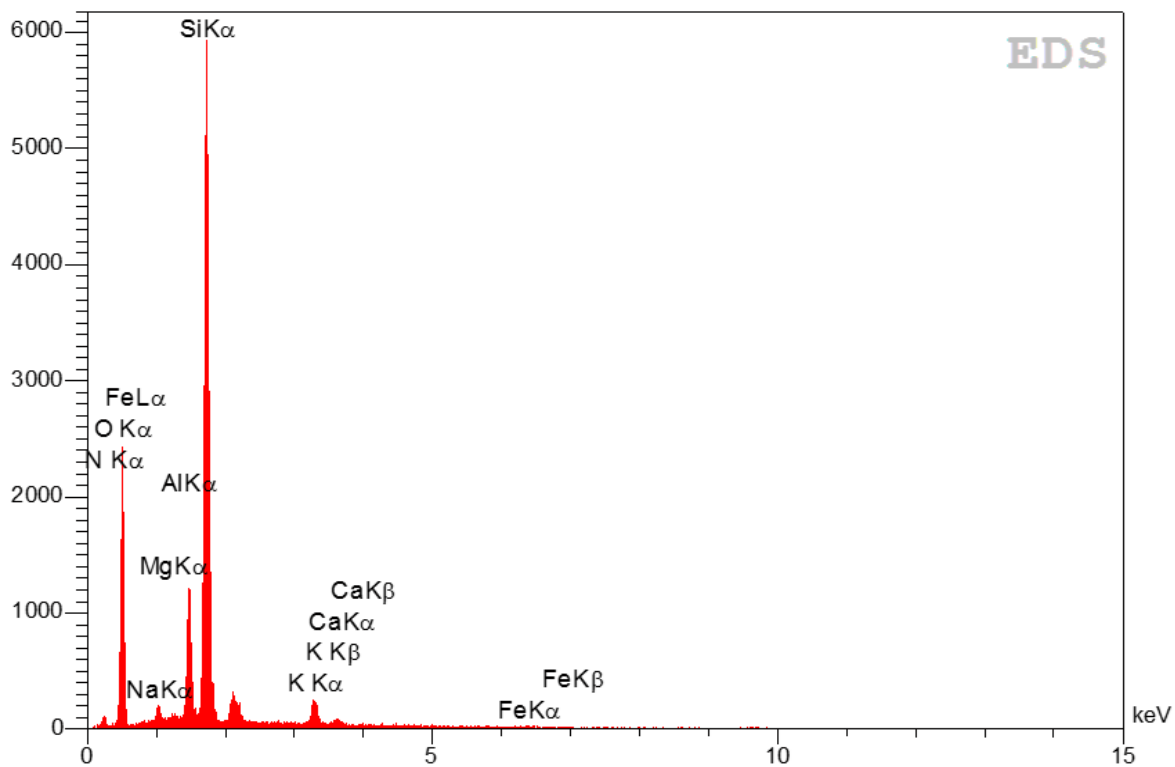


Fig. 6. EDX spectrum of natural zeolite

018  
 019  
 020  
 021  
 022  
 023  
 024  
 025  
 026  
 027  
 028  
 029  
 030  
 031

Accepted in

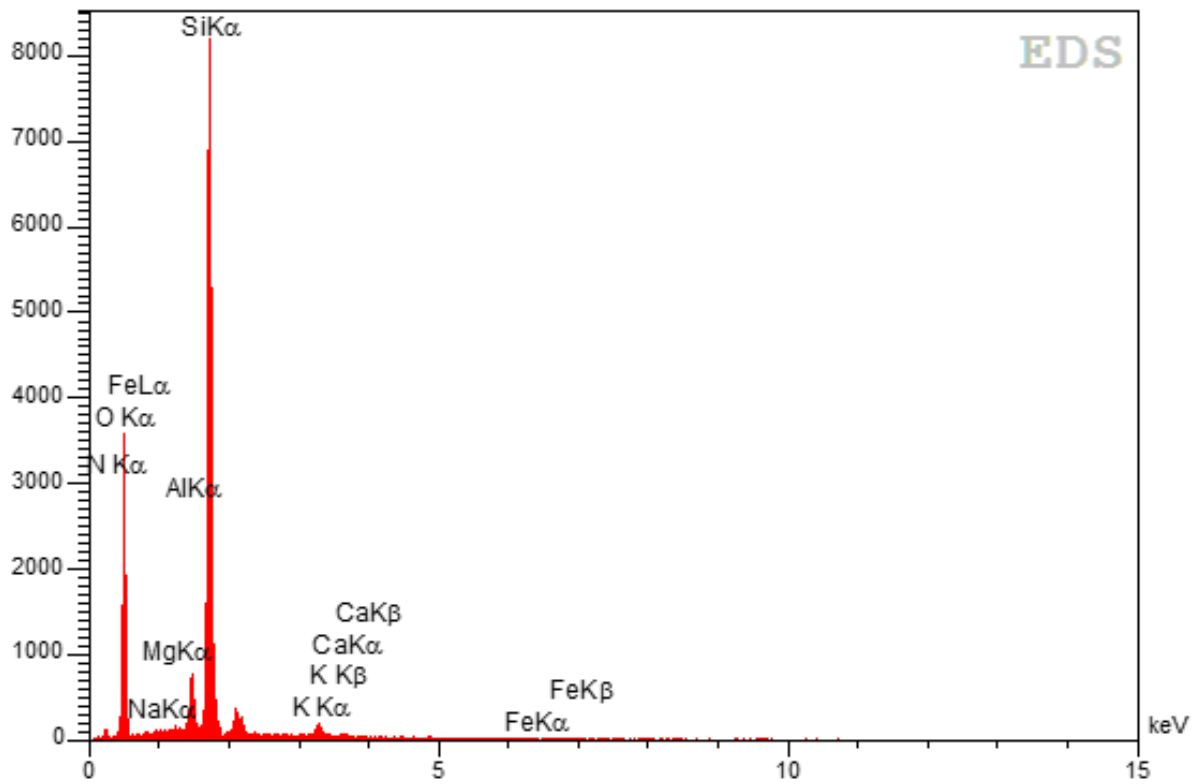
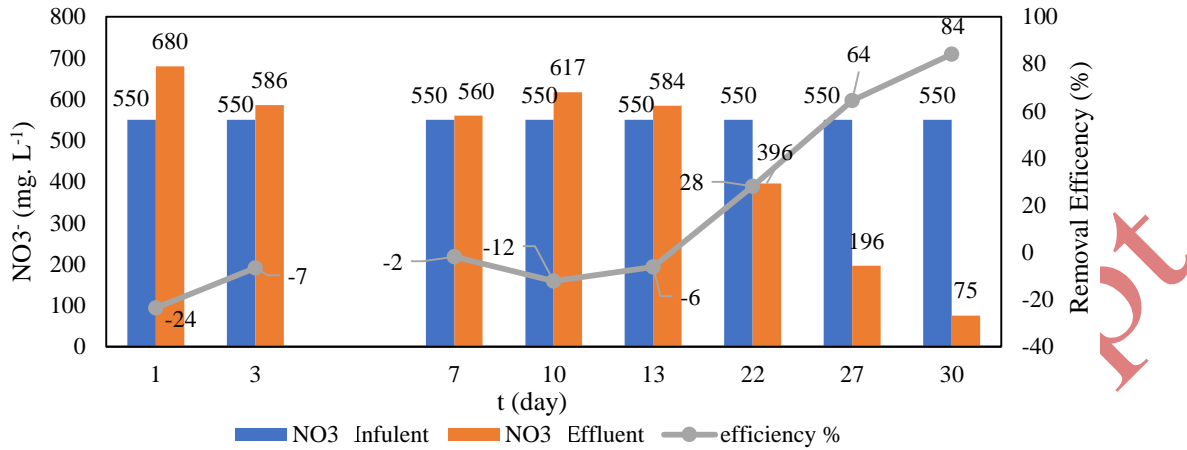


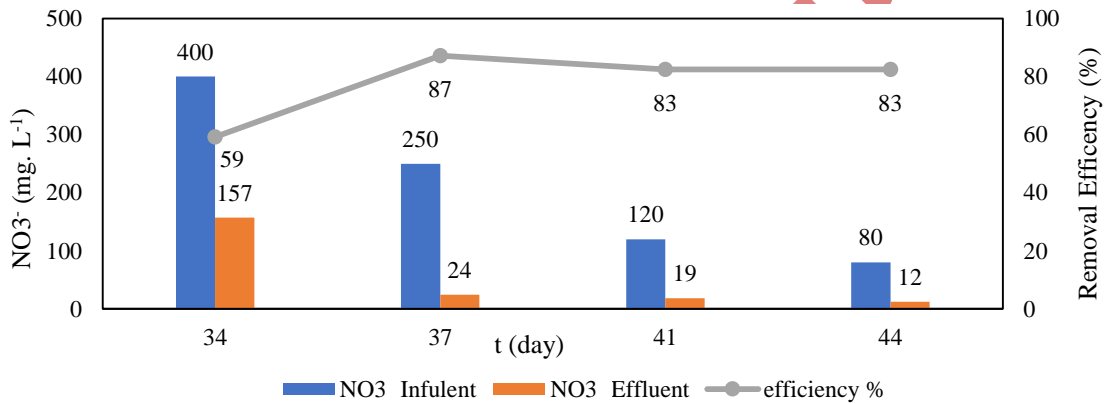
Fig. 7. EDX spectrum of modified zeolite

032  
 033  
 034  
 035  
 036  
 037  
 038  
 039  
 040  
 041  
 042  
 043  
 044

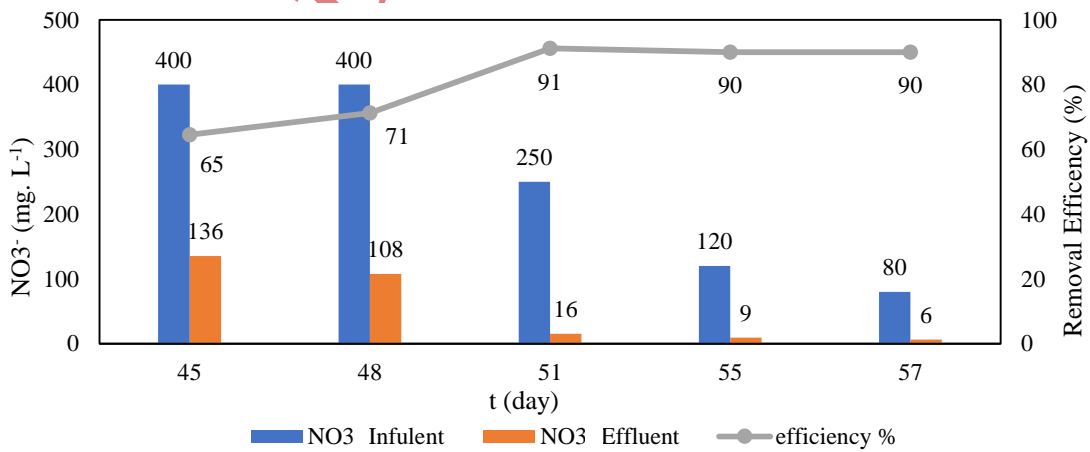
(a) HRT= 25 & 32 Hours



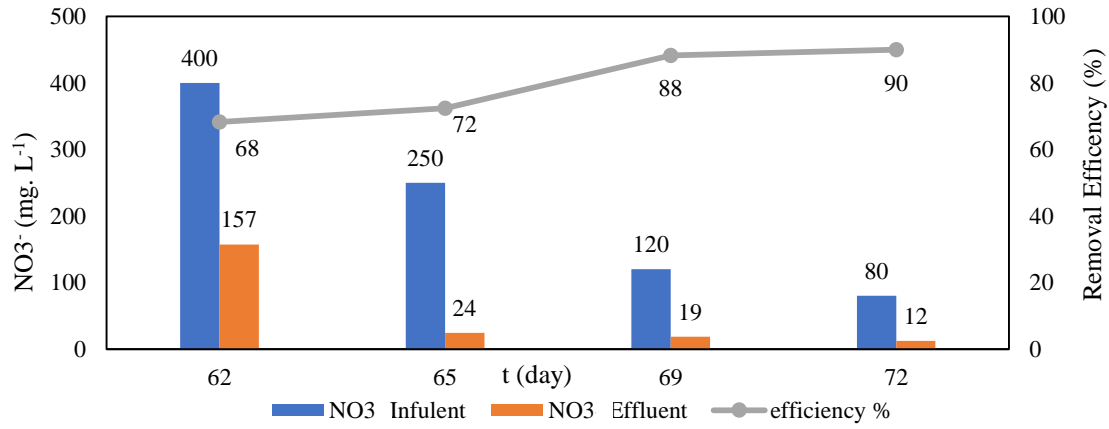
(b) HRT= 25 Hours



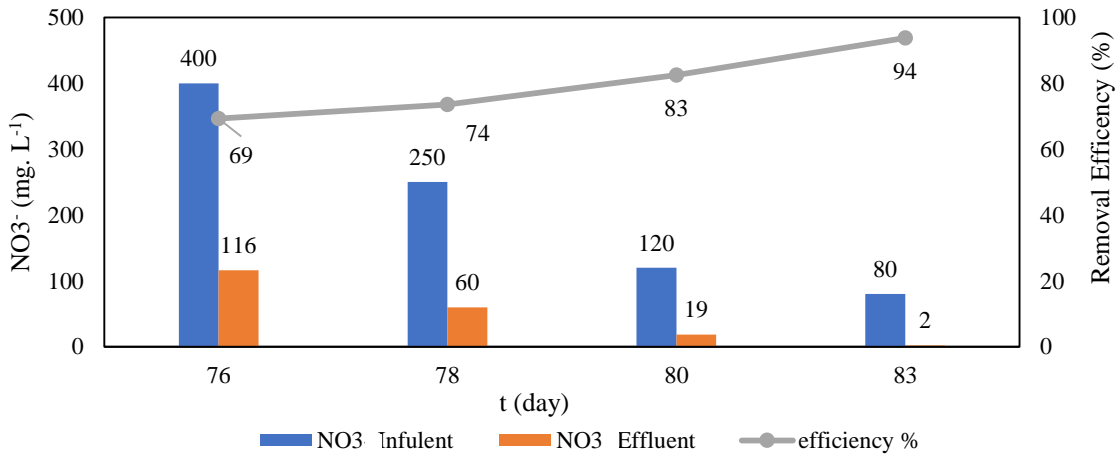
(c) HRT= 15 Hours



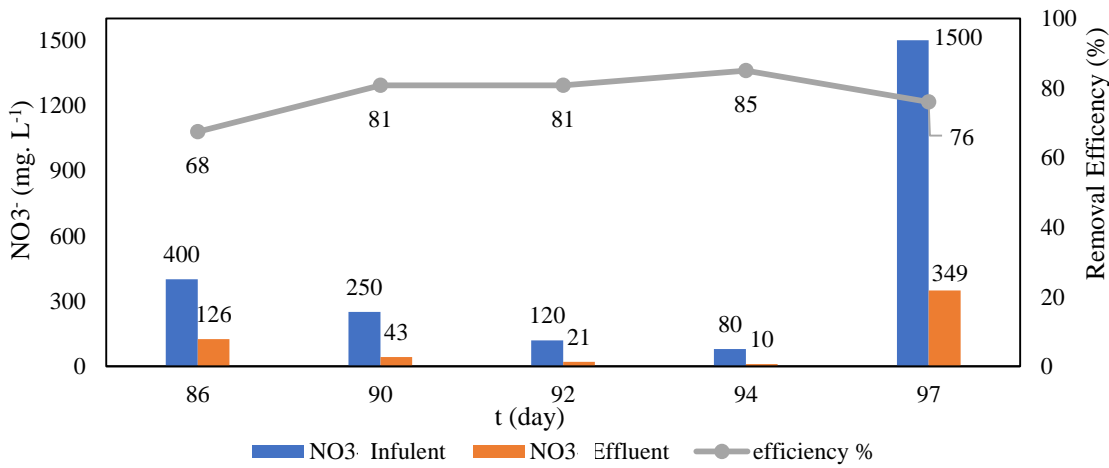
(d) HRT= 12 Hours



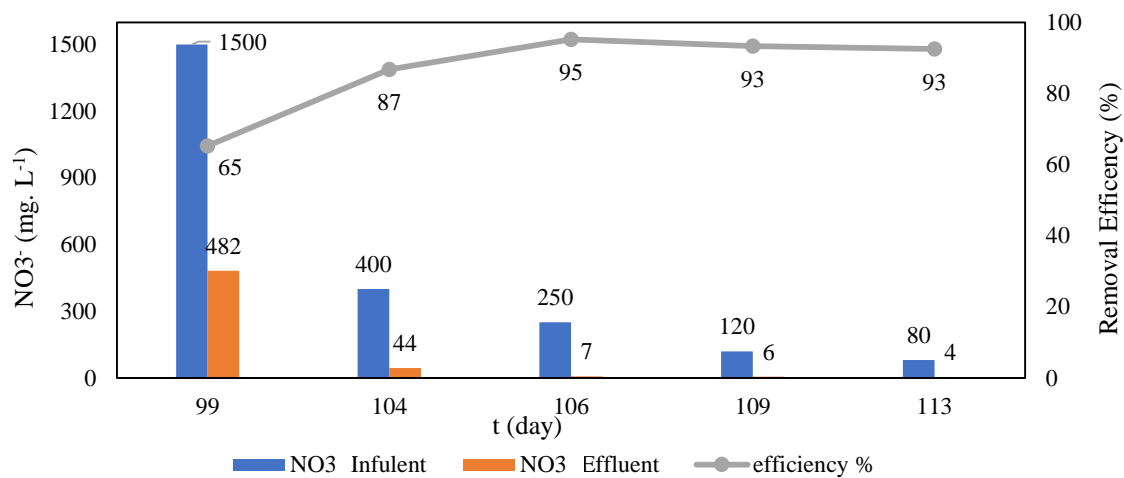
(e) HRT= 10 Hours



(f) HRT= 6 Hours

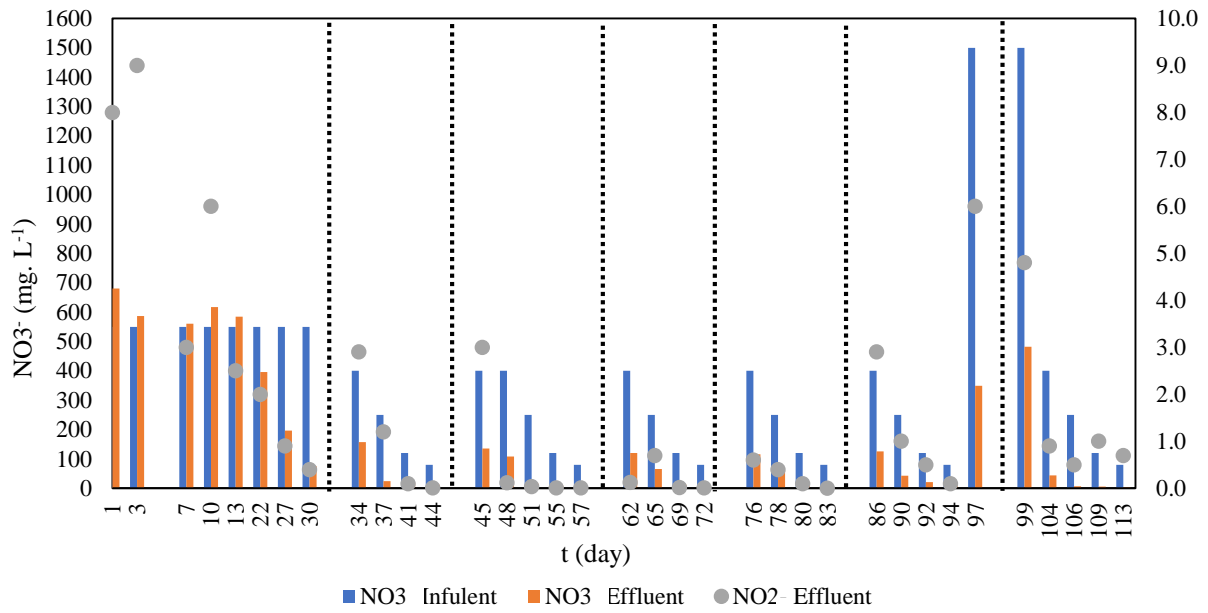


(g) HRT= 3 Hours



040 **Fig. 8.** Nitrate concentration and removal efficiency of the bioreactor for various HRTs, (a) set-up and growth: 25 &  
 046 32 hours, feeding: (b) feeding: 25 hours, (c) 15 hours, (d) 12 hours, (e) 10 hours, (f) 6 hours, (g) 3 hours  
 047

Accepted manuscript



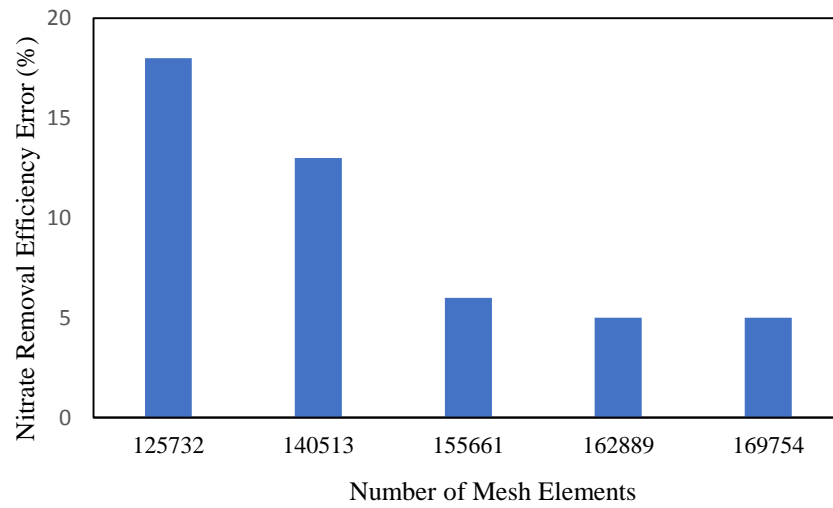
048

049

00.

**Fig. 9.** Concentration of the input nitrate, output nitrate and output nitrite for different HTRs

Accepted manuscript



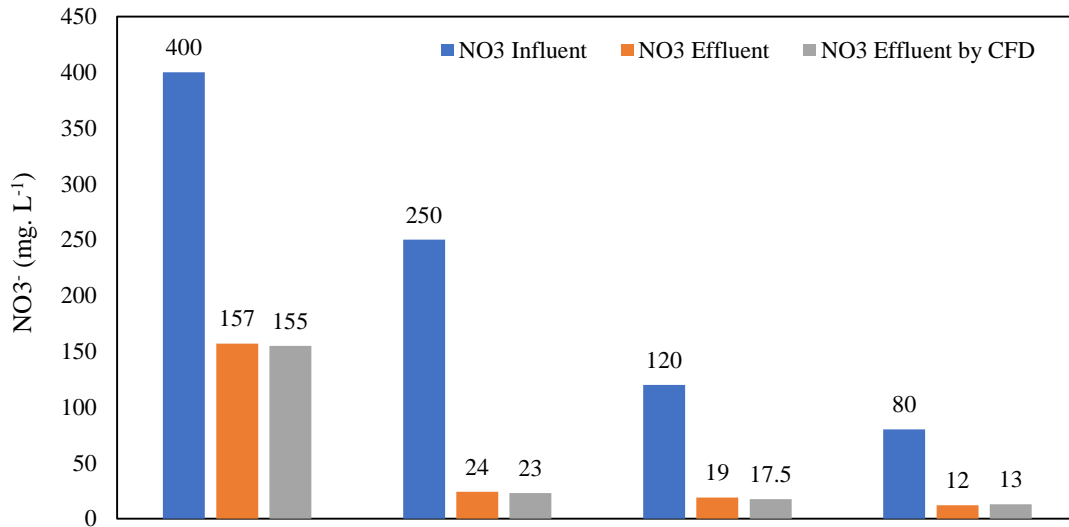
001  
002  
003

**Fig. 10.** Computational error based on different mesh sizes/number of elements

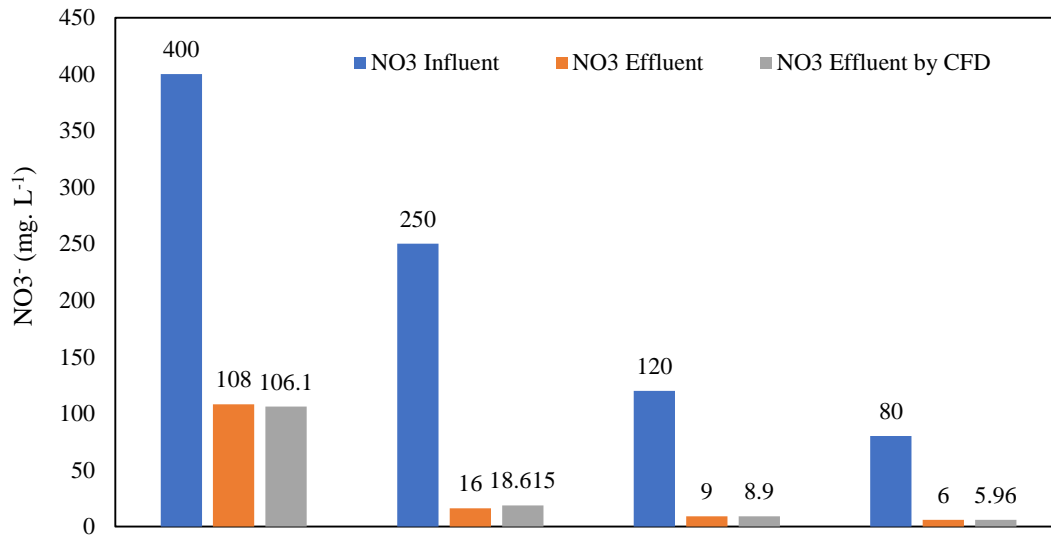
Accepted manuscript



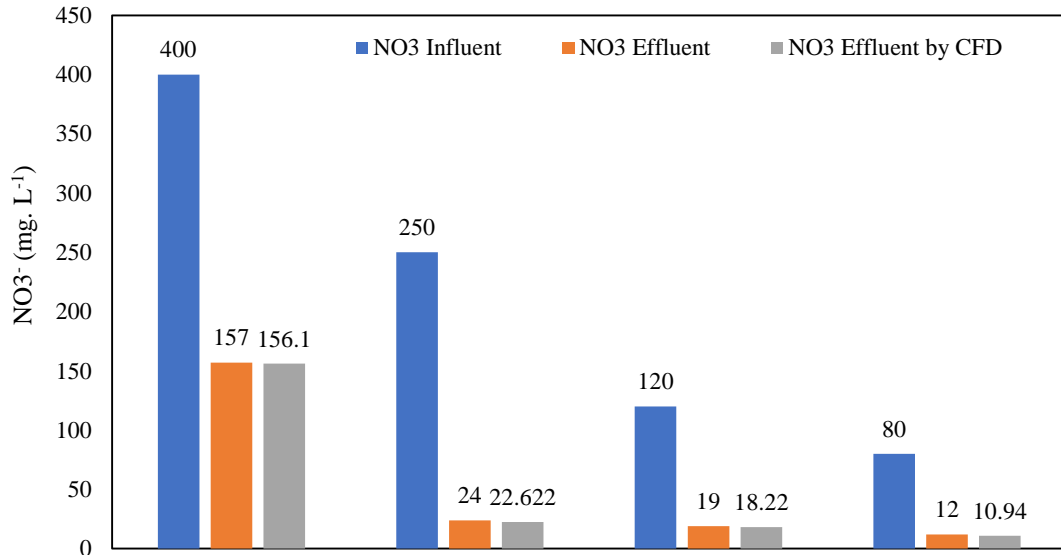
(a) HRT= 25 Hours



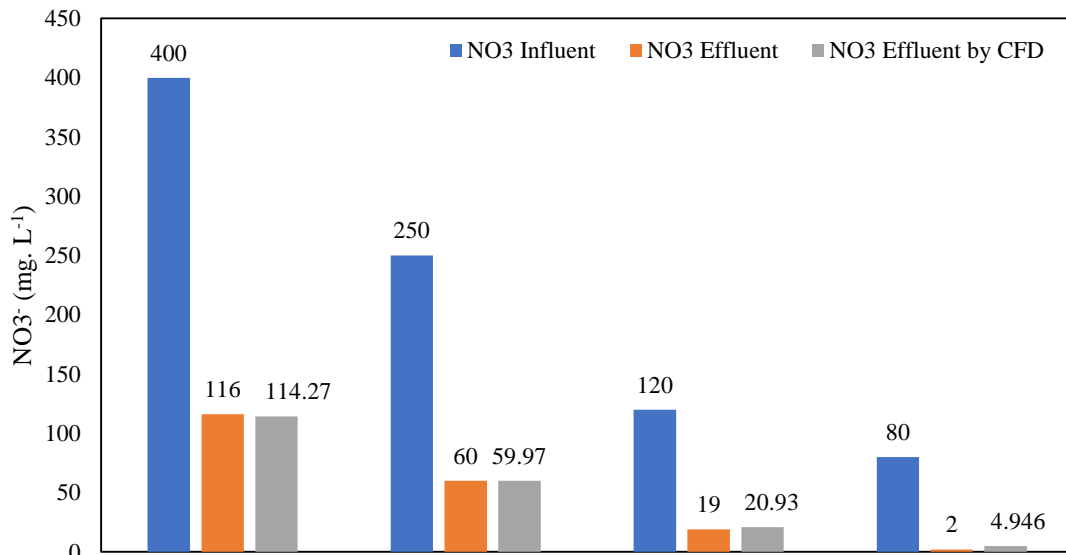
(b) HRT= 15 Hours



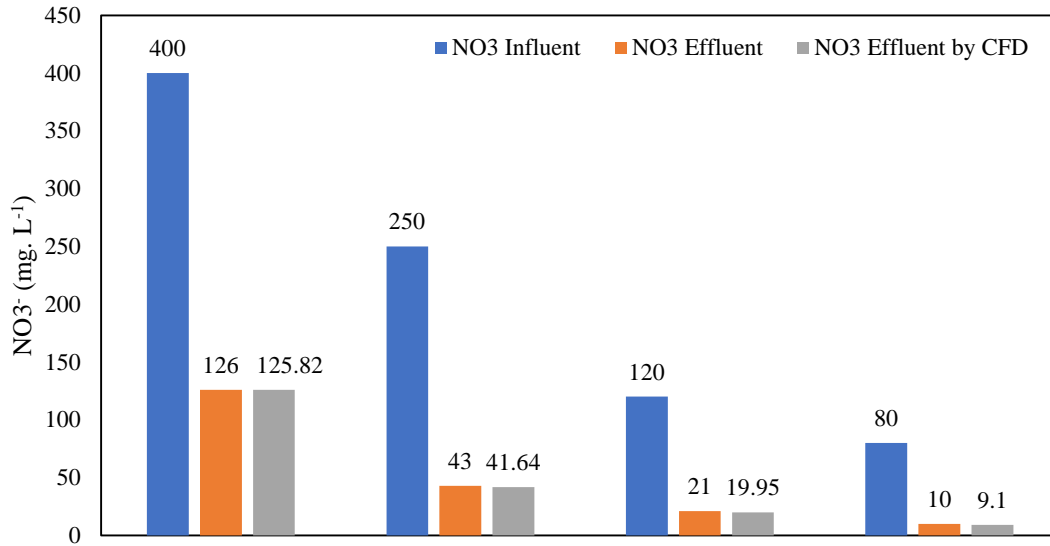
(c) HRT= 12 Hours



(d) HRT= 10 Hours



(e) HRT= 6 Hours



(f) HRT= 3 Hours

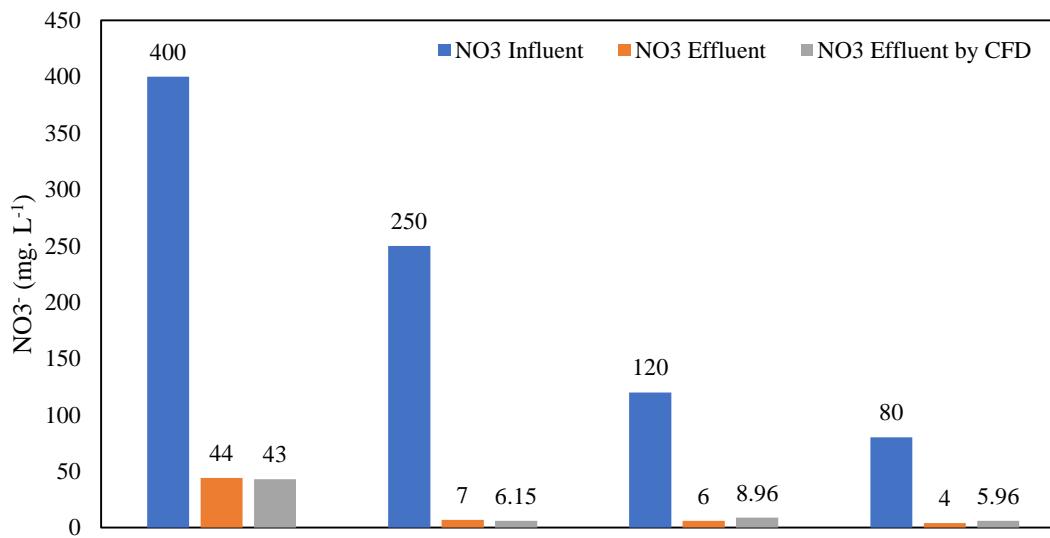


Fig. 11. Comparison of CFD simulation results with experimental measurements

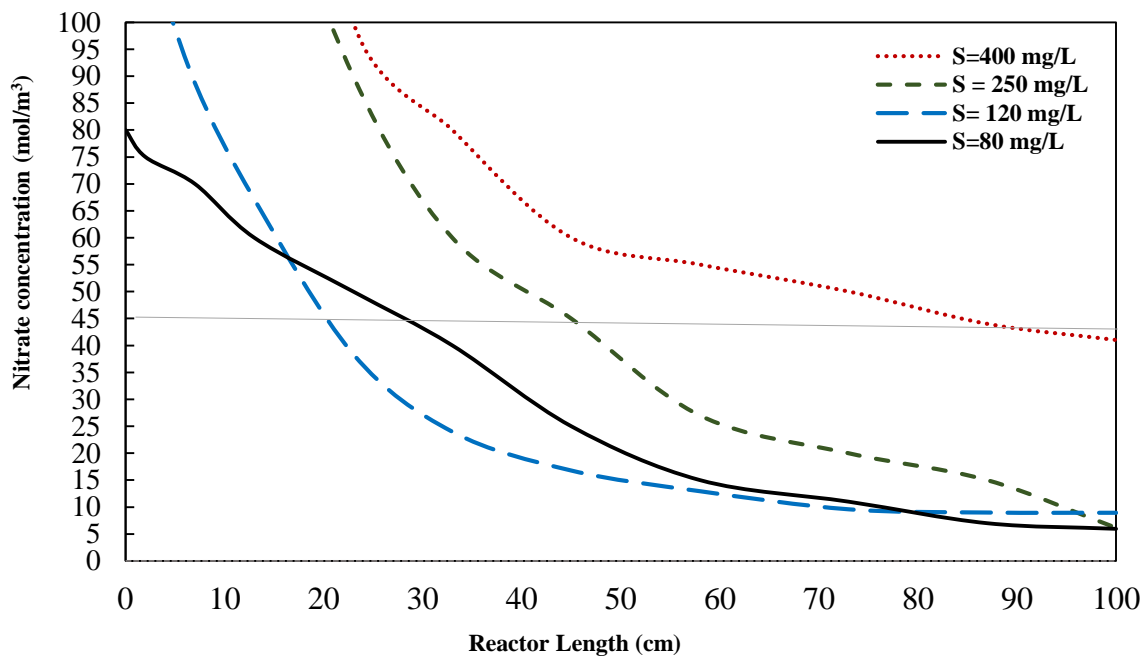


Fig. 12. Nitrate concentration along the bioreactor by simulation, HRT = 3 h

006

007

Accepted manuscript